Experimental study of cyclic behavior of composite vertical shear link in eccentrically braced frames

M.A. Shayanfar[1]*, M.A. Barkhordari[1], and A.R. Rezaeian[2]

*[1]Center of Excellence for Fundamental Studies in Structural Engineering, Civil Engineering Department,
Iran University of Science and Technology, Tehran, Iran*
[2]Department of Civil Engineering, Karaj Branch, Islamic Azad University, Karaj, Iran

Abstract. This paper is an experimental study on the behavior of vertical shear link in normal (steel section with and without stiffener) and composite (steel section with concrete located at the area limited to web and flanges of the section) configurations. This study is mainly aimed to perceive failure mechanism, collect laboratory data, and consider the effect of number of transverse reinforcements on strength and ductility of composite vertical links. There have been four specimens selected for examining the effects of different details .The first specimen was an I section with no stiffener, the second composed of I section with stiffeners provided according to AISC 2005. The third and fourth specimens were composed of I sections with reinforced concrete located at the area between its flanges and web. The tests carried out were of quasi-static type and conducted on full scale specimens. Experimental findings show remarkable increase in shear capacity and ductility of the composite links as compared to the normal specimens.

Keywords: eccentrically braced frame, vertical link, composite link, stiffener, transverse reinforcement, confinement

1. Introduction

Examination and study on Eccentrically Braced Frames (EBFs) has been commenced extensively since 70s. Roeder and Popov (1977) and Ricles and Popov (1987) expressed that EBFs meet very well the two criteria of seismic design, stiffness and ductility, compared to other lateral load carrying systems such as MRF and CBF. These frames show reasonably appropriate stiffness under moderate earthquakes, and behave in a ductile manner under severe earthquakes. As shown in Fig. 1, eccentricity caused in these frames, represented by Parameter "*e*", is the weakest part of the frame and is the main source of the energy dissipation resulted from earthquakes.

The placement of the link is in horizontal and/or vertical configurations. Therefore, there are two general types of Eccentrically Braced Frames, H-EBF and V-EBF. Generally speaking, the advantages of V-EBFs versus H-EBFs are as follow:
- Transfer of nonlinear deformations to outside of storey beam and dissipating the energy in vertical link only.
- Design of the vertical link is conducted for lateral forces only, because the configuration of V-EBF is

* Corresponding author, Ph. D., E-mail: mohsenalishayanfar@gmail.com
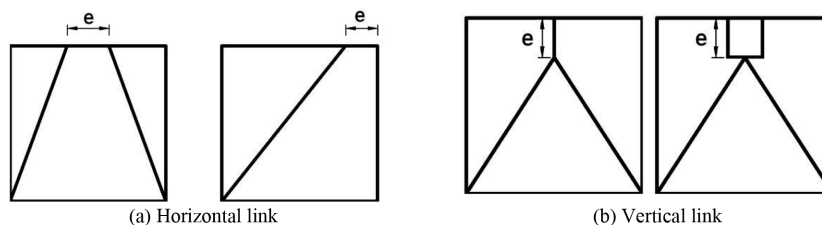
(a) Horizontal link   (b) Vertical link

Fig. 1 Configuration of EBFs

so that inconsiderable force is transferred from gravitational loads to vertical link.

- Simple replacement of vertical link after occurrence of the earthquake, because it is acting out of basic structural lateral resisting system.
- Application in seismic rehabilitation of the existing buildings due to its low cost and easy construction.

The eccentrically braced frame with vertical link was used as a new type of steel braces by Seki *et al.* (1988). They called this system "Y-Shaped Braces". Their studies showed that the system's hysteretic diagram is very stable and symmetric. Having compared the behaviors of Inverted Chevron-V braced frames and Eccentrically Braced Frames with vertical link, Wakabayashi (1989) demonstrated that V-EBFs have more appropriate and stable behavior than that of Inverted Chevron-V braced frames. Based on theoretical studies, Fehling *et al.* (1992) reviewed such a system and made use of the results of the report rendered by Roeder and Popov (1977) in eccentrically braced frames with horizontal link due to lack of information on stability of vertical link region. The report (Fehling *et al.* 1992) emphasized that instability occurs in vertical link as a result of either large deformation or lack of adequate lateral support within the link. The results of their studies also revealed very high ductility and high efficiency for this structural system. Vetr (1998) conducted an experimental studie on a three stories frame to examine the seismic behavior of such a system. The obtained results exposed ductile behavior of the system and the need for a support to be provided in the connection between link and storey beam. Takahashi and Shinab (1995) focused their researches on the use of steel of low yielding tensile strength in the specifications of vertical links. They made use of H-shaped sections with low strength steel web and high strength steel flanges. The results showed more energy dissipation capacity due to the use of mild steel in H-shaped sections. Zahrai and Bruneau (1999) and Sarraf and Bruneau (2000) studied the use of vertical links for vulnerability assessment and rehabilitation of existing bridges. The results of their laboratory investigations showed an increase in ductility of the system and remaining its other components in elastic range. Hysteretic diagrams obtained from their researches revealed a stable behavior for the system under seismic loading. Ghobarah and Abou Elfath (2001) undertook detailed numerical studies of the V-EBF to decrease damages to reinforced concrete structures. The results of their investigation demonstrated the conspicuous effect of such bracing as compared to other systems. Bruneau *et al.* (2002) demonstrated step by step design procedures for the vertical shear links utilized in slab on girder and deck-truss bridges. D'Aniello (2006) used such links as replaceable links in concrete structures and showed the key role of such braces in rehabilitation and retrofitting of existing structures. Shayanfar *et al.* (2008) have commenced new studies on the use of double vertical links in the system whose results have exposed appropriate behavior and added more functional specifications in such structural systems compared with single vertical links.

The most prominent component of the EBFs is the link length. The shorter the link length the higher the effect of the shear force compared to the bending moment, and it is idiomatically said that the frame

behavior is governed by "shear". For the long length of the link, the effect of bending moment increases and the behavior of the frame is referred to as "bending behavior" (Roeder and Popov 1977, Ricles and Popov 1987). The key concern in V-EBFs is on shear behavior rather than bending.

This paper presents an experimental investigation on new proposed details for vertical shear links. This detail utilizes partially encase I or H shape profiles. It is proposed after reviewing the concrete effect on steel members. Uy (2001) concentrated his study on concrete effect in the axial strength in steel and composite columns. The studies of Sherif El-Tawil *et al*. (1999), Chicoine *et al*. (2002), Begum *et al*. (2007) and Szmigiera (2007) on partially encased column had indicated concrete effects on increasing strength and ductility compaired to steel columns. Zhao and Astaneh-Asl (2007) utilized the concrete for preventing the shear buckling and increasing the shear strength in the steel shear walls.

The main purpose of this paper is to achieve an experimental investigation on composite vertical links to obtain a better understanding of the yielding process, failure mechanism in the vertical composite link, to investigate the effect of shear reinforcement spacing on strength and ductility of these links, to compare seismic behavior and shear strength of normal and composite links, and to verify the concrete capability in postponing the web buckling until failure loading.

2. Experimental investigation

This research focuses on experimental study of composite vertical link behaviors. However, numerical analyses are used to determine loading protocol. The proposed details of composite vertical shear links have been shown in the Fig. 2. As per these details, the transverse reinforcements, which play the role of concrete confinement (Mander *et al*. 1988), are welded to web link and responsible for transmission of shear force between web and concrete of the composite section. The longitudinal reinforcements are welded to two ends of the web to prevent their slide movement and the space limited to the web is thoroughly filled with concrete.

2.1. Design and manufacturing of the test specimens

In this section, design (selection of dimensions and length) and construction of the specimens are explained as follow:
Selection of dimensions and link length
Design of specimens has been fulfilled considering the limitations existing in the laboratory. For
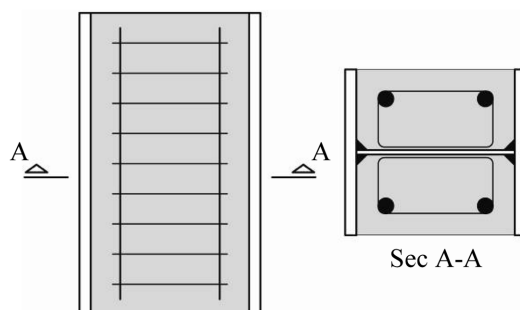

Fig. 2 Proposed details of composite vertical shear link

instance, because the webs of the rolled profiles have actual yield stress higher than their nominal limit (nominal stress is 2400 kg/cm², but the actual stress is 3500 kg/cm²) and in some cases, such webs do not meet the requirements of the code as links (AISC 2005), it was decided to make a plate girder with appropriate specifications for the steel part of the composite link. A plate of actual yield stress of 2490 kg / cm² was therefore used as the link web (this steel is selected from ST33). Since flanges do not play a remarkable role in shear resistance of the link, there is no sensitivity that their yield stress meets a pre-defined limit. Normal steels (ST37) were therefore used for the flanges. Dimensions of the specimens were selected and designed taking numerous parameters into account. Some of these parameters are as follow:

- The existence of enough space between the flange and web of the specimen for reinforcement and concrete.
- The existence of enough web thickness to connect transverse reinforcement.
- The weld between web and flange can bear the stress resulted from shear yielding and strain hardening of the web.
- The weld between the specimen and the plates at the two ends, which are used for connection to strong floor and loading beam, can bear the forces applied until the end of the test.
- Shear behavior is being guaranteed in the link

Given the above mentioned items, a plate girder was designed within the limits of wide-flange beam with the specifications illustrated in Fig. 3.

The important point for design of such a link is to select an appropriate length, because, the link should be able to withstand nonlinear deformations without instability. Therefore, shear hinge was formed in the link due to exertion of lateral forces on the frame. This can introduce maximum loading capacity to the link by combination of isotropic and kinematic hardening properties. Considering the behavior of shear hinge in the horizontal links, where the values of shear and bending moment in the link reach $1.5V_p$ and $1.2M_p$, respectively, owing to strain hardening, and by writing the link equilibrium equations (the amounts of moments at two ends of these two links are equal), the horizontal link length would be obtained by Eq. (1) (Roeder and Popov 1977, Ricles and Popov 1987)

$$e \leq \frac{2 \times 1.2 M_p}{1.5 V_p} = 1.6 \frac{M_p}{V_p} \qquad (1)$$

Where M_p and V_p are plastic moment and shear force, respectively .To have a conservative relation to meet shear behavior, a link length formula has been suggested according to Eq. (2), (Kasai and Popov 1986)
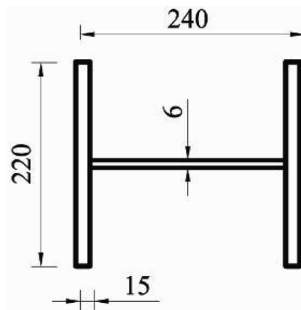

Fig. 3 Dimensions of specimens (Unit: mm)

$$e \leq 1.4 \frac{M_p}{V_p} \tag{2}$$

The most important characteristic of frames with vertical links is non-equality of the two end moments of the links as a result of non-equality of the stiffness of the floor beam and the bracing members, Fig. 4.

Considering the fact that moments at the two ends of vertical links are not equal and taking strain hardening into account as common in horizontal links, vertical link length is determined as Eq.(3)

$$e \leq \frac{1.2 M_p (1 + \kappa)}{1.5 V_p} = \frac{0.8(1 + \kappa)M_p}{V_p}, \; \kappa = \frac{M_2}{M_1} \tag{3}$$

Where, M_1 and M_2 are the top and bottom vertical link moments, respectively.

In order to present a conservative relation with regard to the philosophy used in Eq. (2), the length of vertical shear links is proposed as Eq. (4)

$$e \leq \frac{0.7(1 + \kappa)M_p}{V_p} \tag{4}$$

The length of vertical link can be more reduced in order to decrease moment value at the connection of vertical link to storey beam (connection of link to the Lab strong floor) and to decrease the possibility of the weld failure, like what happens when connecting shear link to column (Kasai and Popov 1986). Reducing the upper moment to half of the plastic moment (0.5 Mp) (Vetr 1998), the link lengths of the test specimens are obtained from Eq. (3) as showed in Eq. (5)

$$e \leq \frac{0.7(1 + \kappa)(0.5M_p)}{V_p} = \frac{0.35(1 + \kappa)M_p}{V_p} \tag{5}$$

It is noteworthy that in this research the length of the links is generally obtained using Eq. (5) regardless of their composite property. If k becomes zero (which is the most critical case), then by substitution of the equivalent values in Eq. (5), the limits of vertical link length to satisfy shear conditions will then be equal to: $e \leq \frac{0.35 \times 808 \times 3000}{0.6 \times 21 \times 0.6 \times 2490}$ = 50 cm. Accordingly the links' lengths were selected to be equal to 40 cm.
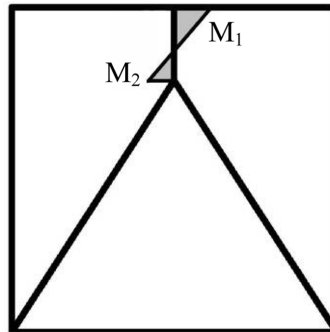

Fig. 4 Bending distribution resulting from lateral force for V-EBFs

2.1.1. Specification of specimens

Four specimens tested in this research program.

Specimen 1: Vertical Steel Link with no Stiffener (VSL1)

This specimen simulated the behavior of a vertical steel link without stiffener. The details of this specimen showed in Fig. 5.

Specimen 2: Vertical Steel Link with Stiffener (VSL2)

For this sample, stiffeners were designed according to AISC 2005 seismic provision code (AISC 2005). Considering the design details, two stiffeners, $210 \times 107 \times 10$ mm, at distance of 135 mm, should be mounted on one side of the link, Fig. 6.

In order to decrease the hydrostatic stress in link web, the weld between stiffener and link web was stopped 3tw (tw is web thickness) from the flange to web connection (McDaniel *et al.* 2003).

Specimens 3 and 4: Composite Vertical Links (CVSL1 and CVSL2)

The intended composite links are constructed based on the details of Fig. 2, and their transverse and vertical reinforcements are $\phi 8$ and $\phi 20$, respectively. In this research two composite samples whose difference was in the distance between their transverse reinforcements. The distances between transverses reinforcement (a) are 40 mm and 80 mm in CVSL1 and CVSL2, respectively.

It is noteworthy that the transverse reinforcements were placed alternatively in both sides of the samples to prevent any possible brittle failure caused as the result of weld on web at a point with the same distance from both sides as illustrated in Fig. 7. This figure shows the details of the composite specimens.

Specifications of all specimens are summarized in Table 1. The descriptions of all materials used in the specimens listed in Table 2.
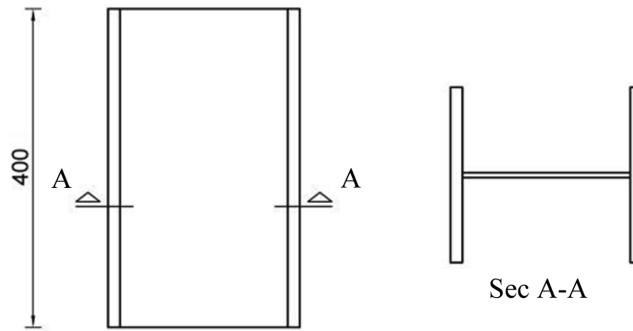
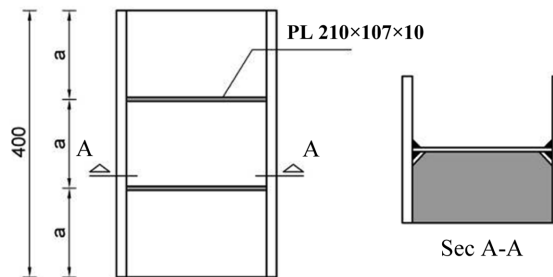

Fig. 5 Detailing of Specimen 1 (Unit: mm)
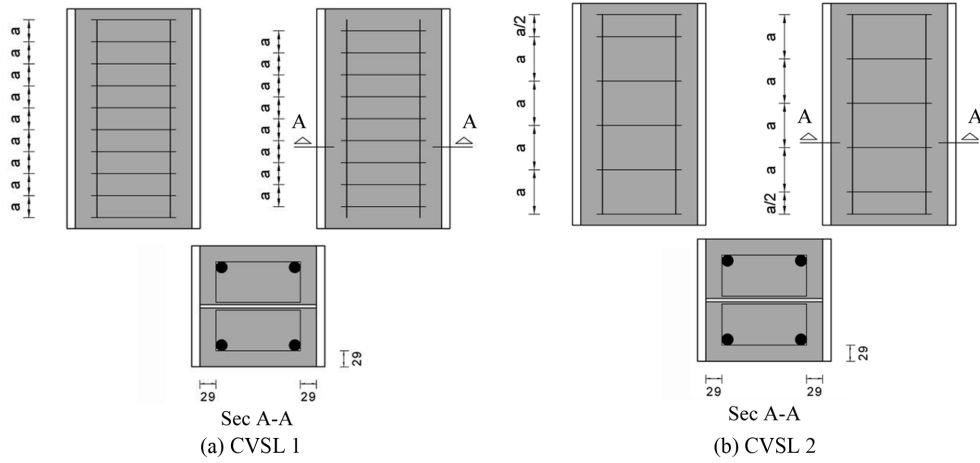

Fig. 6 Detailing of Specimen 2 (Unit: mm)

Fig. 7 Composite specimen (Unit: mm)

Table 1 Parameters of the specimens

Name	Length mm	No. Stiffener	a mm	Description
VSL1	400	---	---	Normal
VSL2	400	2	135	Normal
CVSL1	400	---	40	Composite
CVSL2	400	---	80	Composite

Table 2 Properties of the specimens materials

Material	F_y Pa	F_u Pa	f_c Pa
Web steel	249	370	---
Flange steel	300	400	---
Transverse rebar	400	600	---
Concrete	---	---	25

2.1.2. Construction procedure

As mentioned earlier, a plate girder was used for steel part of the vertical link. Submerged arc welding was used to make such a plate girder. Shielded metal arc welding was used to connect transverse reinforcements to the web. Weld used to connect flanges and webs to upper and lower plates are groove weld with complete permeability and fillet weld, respectively. Fig. 9 shows the construction details of the composite links.

2.2. Test setup and instrumentation

Due to the fact that the entire shear story is absorbed by the link in V-EBFs, Fig. 9, and other structural members are supposed to be remained in the elastic region, the frame nonlinear behavior is concentrated in the vertical link. It is noteworthy that such theory is thoroughly true if only the stability of the whole
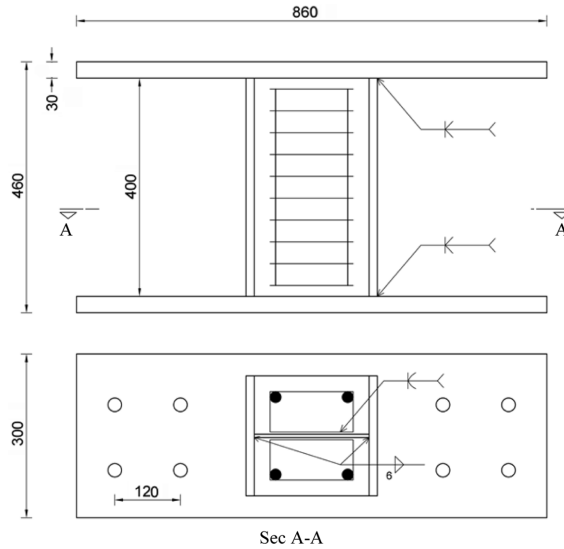
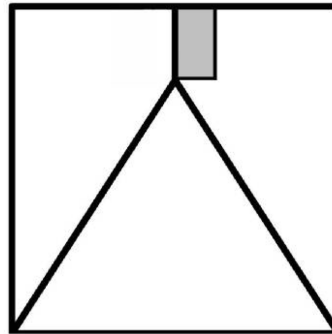Fig. 8 The details of construction layout (Unit: mm)

Fig. 9 Shear distribution resulting from lateral force for V-EBFs

frame is provided. Numerical and experimental studies have proved the stability of the whole frames (Vetr 1998). In this regard, boundary conditions similar to that of the vertical links were developed and the links were tested out of the frame.

As mentioned above, the most important characteristic of frames with vertical links is non-equality of the two end moments of the links as a result of non-equality of the stiffness of floor beam and the bracing members, Fig. 3. Most of the times, the stiffness of floor beam is much higher than that of braced members. Therefore, the link moment developed near the storey beam is larger than the moment adjacent to the braced members.

To simulate such conditions in laboratory, one end of the link is connected to the strong floor and the other end is connected to a loading beam with much lower stiffness than that of laboratory strong floor. A plate, with 30 mm thickness and 860 mm length, was used to connect the specimens to the strong floor. To prevent the rotation of the two link ends, two short columns and a horizontal beam accompanied four rollers at the two ends of the loading beam were utilized, Fig. 10.
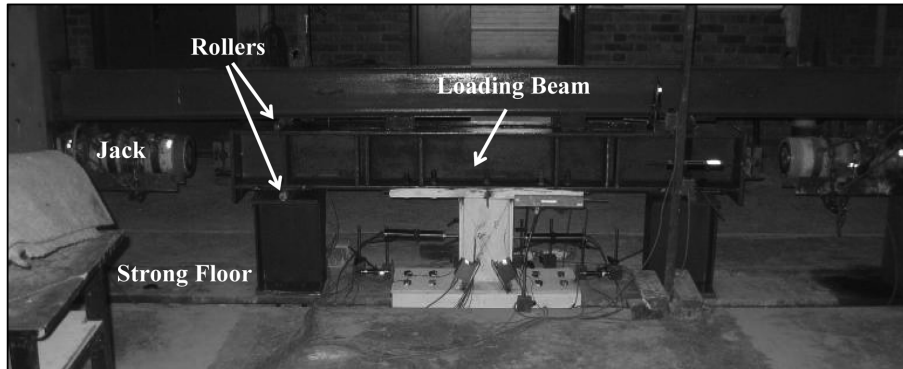
Fig. 10 Test set-up

ATC24 (ACT 1992) was used to schedule the loading history in these tests. It should be mentioned that in some previous tests programs conducted by other researches on EBFs (link only or whole frames) the loading protocol from AISC seismic provision 2002 (AISC 2002) has been adopted (Itani 1997, Dusicka *et al*. 2002, Okazaki *et al*. 2005). This loading protocol has been revised in AISC seismic provision 2005 based on the latest research findings related to short link in EBFs (Richards and Uang 2006). This protocol has been presented particularly for testing the connection between link and column. In the meanwhile, the use of ATC24 protocol was recommended by commentary of AISC seismic provision 2005. Therefore in this study was used the ATC24 protocol. According to ATC24, loading up to the specimen yielding point was conducted by force control and beyond this limit by displacement control. Capacity curves, obtained from a nonlinear analysis under monotonic loading using ANSYS11 (ANSYS User's Manual 2006) software, were used as a landmark; and the information obtained from the strain gages mounted on the link web were used during the test. Considering the fact that the first test was conducted on VSL1, loading protocol was established for this test, and was followed in all tests to facilitate the comparison among the results of different specimens. In the following, a method for determining the protocol is explained. Finite element model for specimen 1 (VSL1) together with the capacity curve were shown in Fig. 11. As shown in the figure, the specimen has yielded at the displacement of 1.6 mm. This point was examined within the test by continuously reading of the numbers obtained from the web strain gages. At the end, the utilized
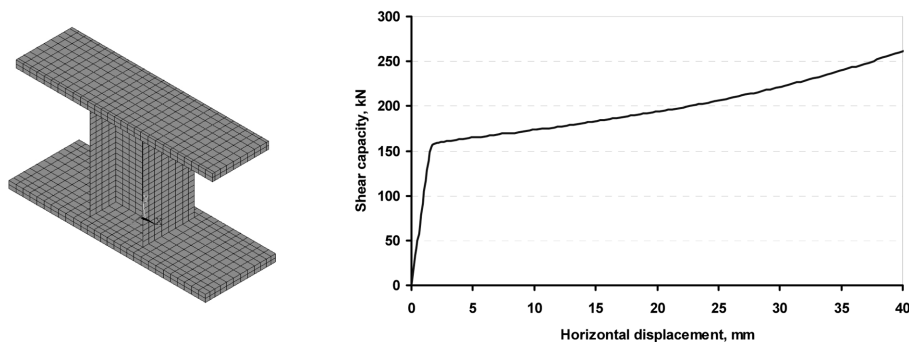

Fig. 11 Finite element modeling of specimen 1

loading protocol has been established as shown in Fig. 12.

Load Cells, LVDTs and strain gages were used to record the data resulted from the tests including applied loads, displacements and strains. Linear and rosette types strain gages were mounted on specimen flanges and web, respectively. Several LVDTs in different places of the prototype were used to record the displacements occurred. Two load cells with 100 tons capacity were also mounted to record the load applied in subsequent loading cycles. Fig. 13 shows the strain gauge installed in Sample 2. Fig. 14 shows the arrangement of LVDTs and Table 3 explains the role of each LVDT.

3. Experimental observations

This section describes the observations and experimental findings. In Figs. 15 and 16, Specimen 1(VSL1) has been shown at yielding and rupture stages, respectively. This specimen yielded at the displacement of 0.16 mm (cycle No.3) and began to rupture through the middle of the shear panel in cycle No. 26 at displacement of 25 mm. Hysteresis Diagram of specimen 1 has been shown in Fig. 17.

In Figs. 18 and 19, Specimen 2(VSL1) has been shown at yielding and rupture stages, respectively. This specimen yielded at the displacement of 0.16 mm due to the fact that the yielding displacement of this specimen was equal to the Specimen 1. In cycle No.38, at the displacement of 32 mm the specimen began
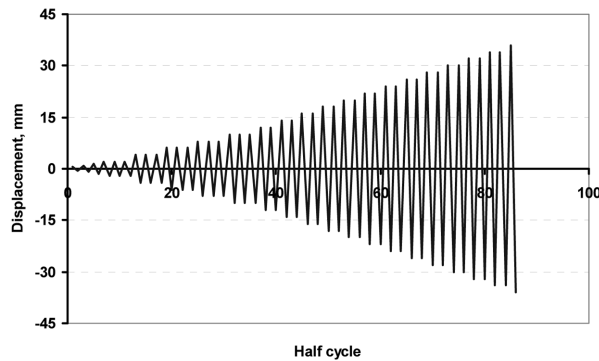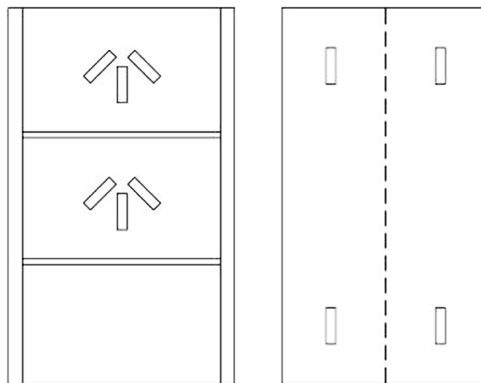

Fig. 12 Loading protocol

Fig. 13 Location of strain gages on the specimen 2

Fig. 14 Location of LVDTs on all specimens

Table 3 Numbers of LVDTs and their role

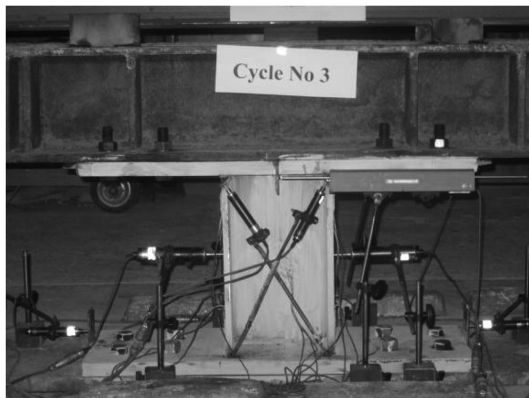| LVDT Number	Role	LVDT Number	Role
2	Record of lateral dis.	6	Record of slip
3	Record of lateral dis.	7	Record of slip
4	Record of lateral dis.	10	Record of slip
5	Record of lateral dis.	11	Record of slip

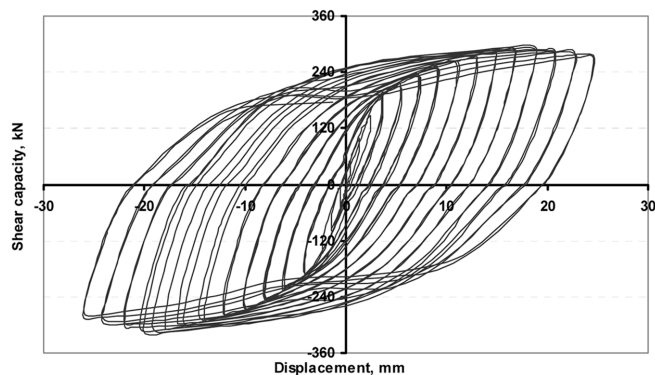Fig. 15 Web yielding in specimen 1

Fig. 16 Web rupture in specimen 1

Fig. 17 Hysteresis diagram of specimen 1

to fail from the place of upper stiffener. Hysteresis Diagram of the specimen 2 has been shown in Fig. 20.

In Figs. 21 and 22, Specimen 3(CVSL) has been shown at cycle number 23 and rupture stages, respectively. In this Specimen, the concrete began to crack at cycle 8 at displacement of 0.6 mm. Meanwhile, at the cycle of 21 the concrete shell was spalled and the confined concrete contributed in bearing the load. Hysteresis Diagram of this specimen has also been shown in Fig. 23. In cycle 42 at displacement 38 mm the web adjacent to the flange and parallel to the stiffener started rupturing.

In Figs. 24 and 25, Specimen 4(CVSL2) has been shown at cycle number 23 and rupture stage. In this Specimen, the concrete began to crack at the cycle 7 at displacement of 0.6 mm. Meanwhile, at the cycle of 18 the concrete shell was spalled and the confined concrete contributed in bearing the load. Hysteresis diagram of this specimen has been shown in Fig. 26. In cycle 40 at displacement 36 mm the web adjacent to the flange and parallel to the stiffener started rupturing.

Fig. 27 illustrates a comparison of hysteretic diagram of VSL1 and VSL2, both diagrams are coincided before web buckling. Fig. 28 shows a comparison of hysteretic diagrams of VSL1 and CVSL1. The composite specimen 3 (CVSL1) reveals significant increase in shear strength and ductility compared to specimen 1, while the stiffness of the two specimens remains approximately the same. Fig. 29 shows a comparison of hysteretic diagrams of VSL2 and CVSL1.
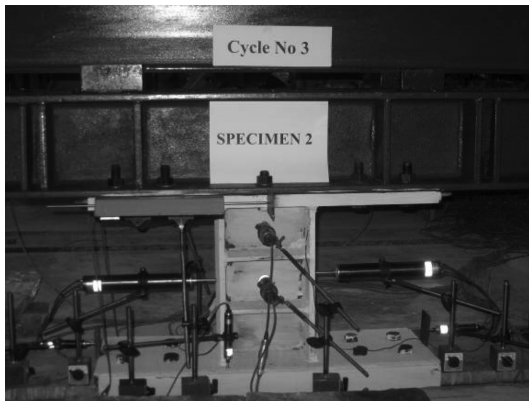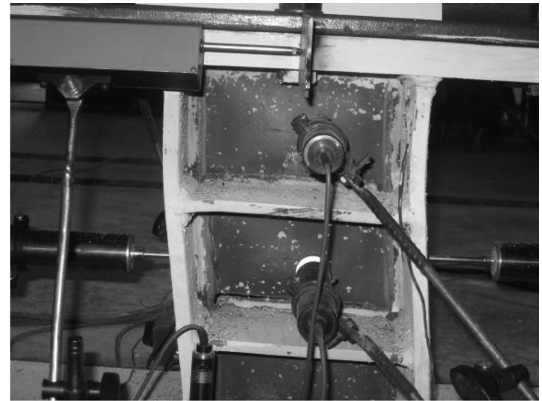

Fig. 18 Web yielding in specimen 2

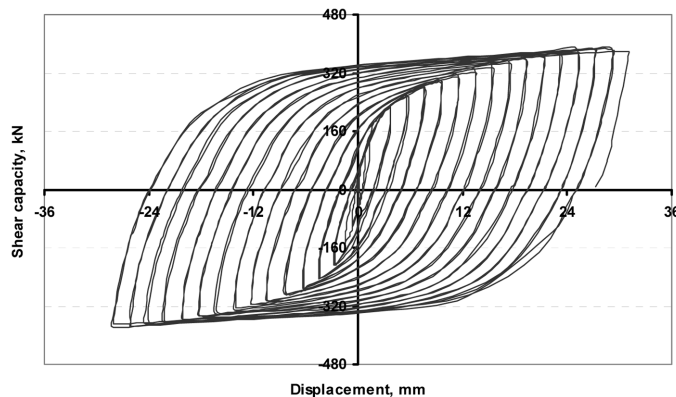Fig. 19 Web rupture in specimen 2

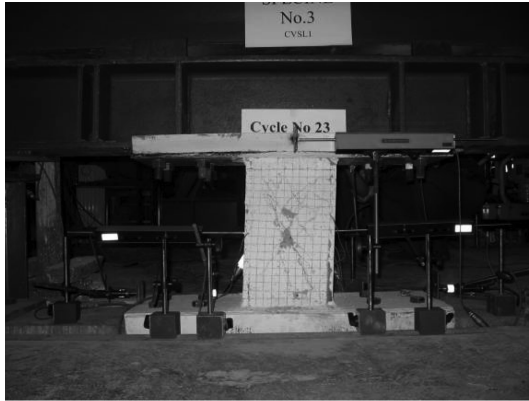Fig. 20 Hysteresis diagram of specimen 2

Fig. 21 Crack progressive in specimen 3
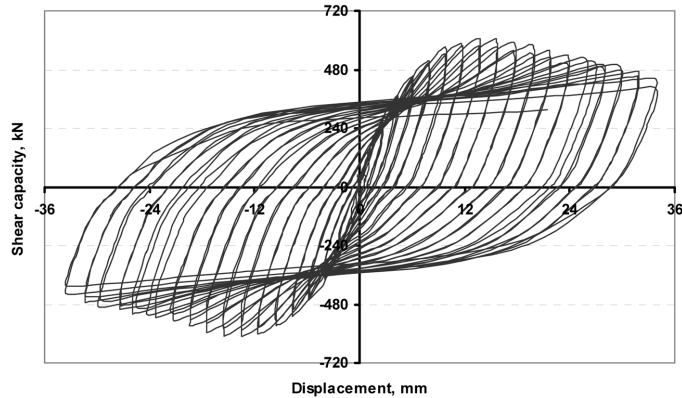

Fig. 22 Web rupture in specimen 3

Fig. 23 Hysteresis diagram of specimen 3

In Figures 30(a) and 30(b), the capacity and over strength factor curves for all specimens are shown, respectively. The over strength factor is defined as shear strength divided by yielding shear force for each specimen. Figure 30(a) illustrates that the yielding force for specimen CVL1 is approximately two times the corresponding value for specimen VSL1. The over strength factors for VSL1 and CVSL1 are equal up to shear strain of 0.04 radian. This factor is 2 and 1.4 for VSL1 and CVSL1 at shear strain 0.08, respectively. This problem imposes limitation on use of ordinary link elements for areas with high seismic demands.

The dissipated energy for specimens VSL1 and CVSL1 versus test cycles and their cumulative plastic strains are displayed in Figures 31(a) and 31(b), respectively.

4. Concluding remarks

This paper presented an experimental study examining the hystesis behavior of vertical link in normal and composite configuration. Four full scale specimens were tested in quasi static.

The hysteresis diagrams of specimens 1 and 2 are coincided before shear plastic buckling; but there is a significant decrease in shear strength and stiffness for the first specimen after shear buckling. The
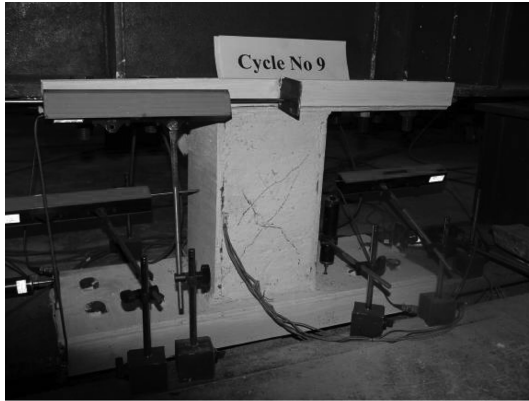
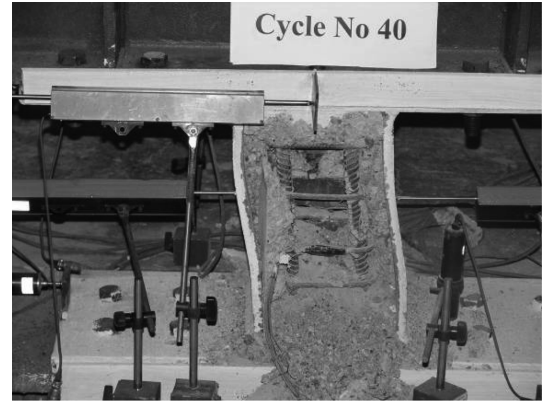Fig. 24 Initial crack in specimen 4
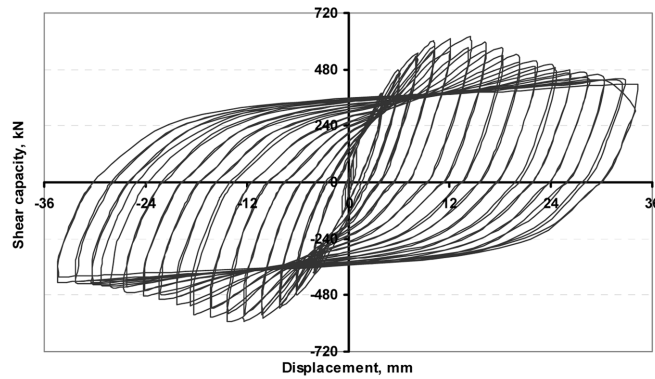

Fig. 25 Web rupture in specimen 4
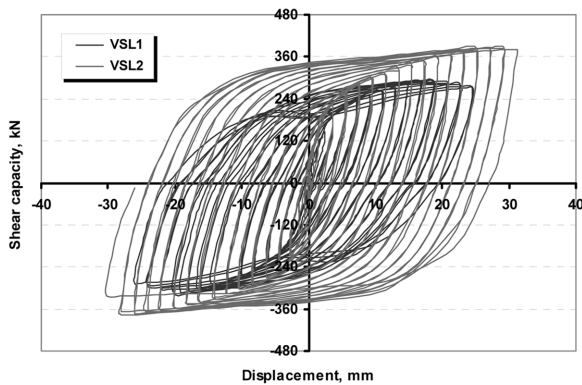

Fig. 26 Hysteresis diagram of specimen 4

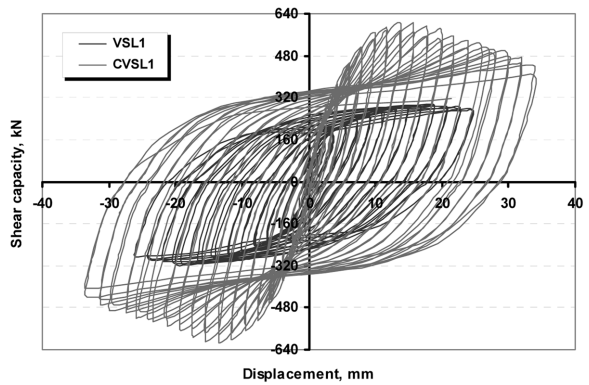Fig. 27 Comparison between hystersis characteristics of specimen 1 and 2

Fig. 28 Comparison between hystersis characteristics of specimen 1 and 3

existence of stiffeners causes the web shear buckling to be postponed and plays an important role in the increase of the specimen ductility. At the rotation of 0.08^{rad}, the web of specimen 2 began to rupture at the
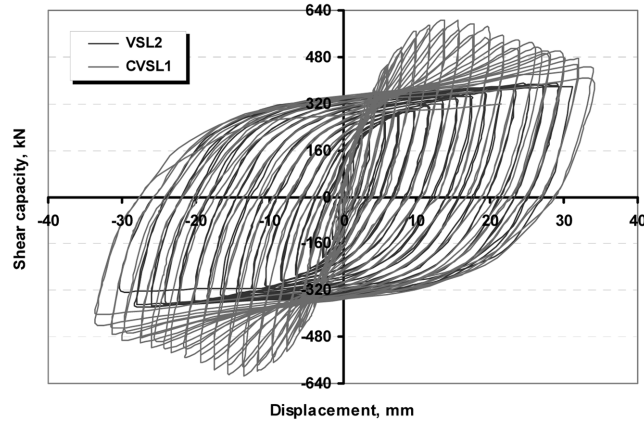
Fig. 29 Comparison between hystersis characteristics of specimen 2 and 3

(a) Capacity curve

(b) Over strength factor curve
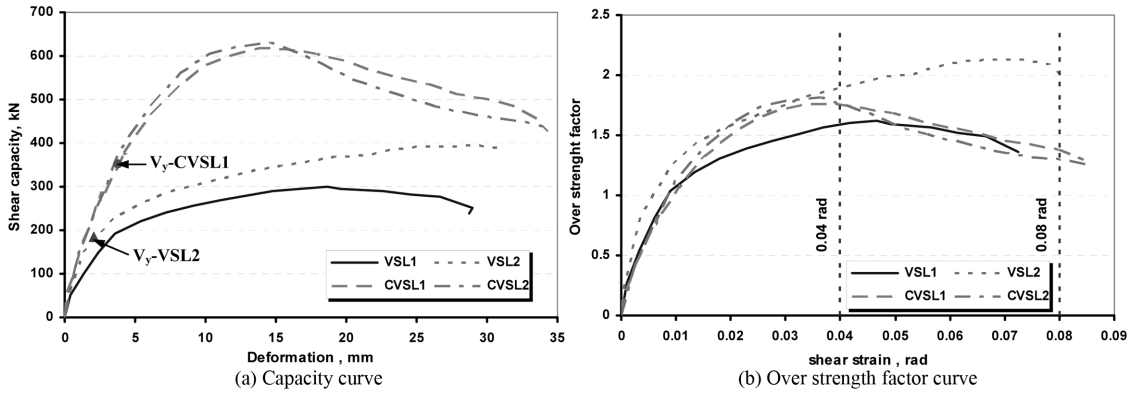
Fig. 30 Comparison among capacity and over strength factor curve of all specimens

(a) Dissipated energy versus cycle

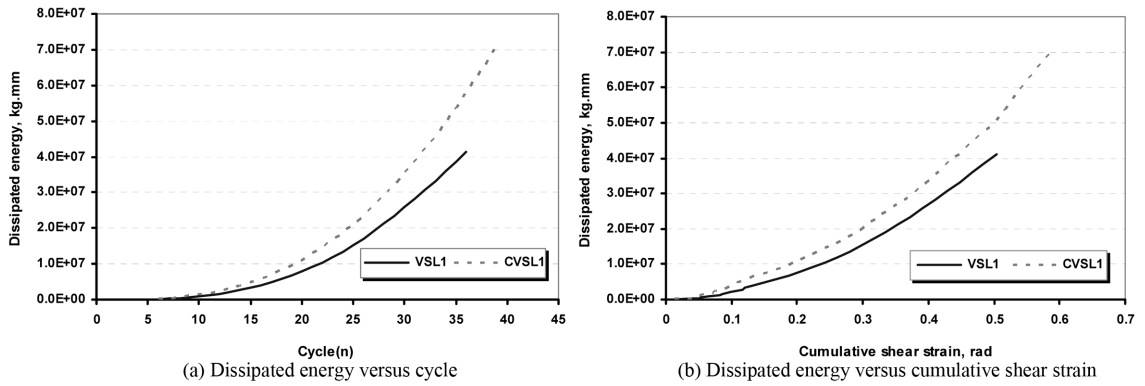(b) Dissipated energy versus cumulative shear strain

Fig. 31 Comparison between dissipated energy of VSL1 and CVSL1

location of upper stiffener due to stress concentration. The second specimen demonstrated a significant strain hardening about 2.

The proposed details for composite vertical link caused an increase in shear strength and dissipated energy up to 100 and 38.4 percents, respectively. By comparison between hysteresis diagrams and capacity curves of samples 2 and 3, it is concluded that the two specimens have the same behavior at the last loading cycles, in which the concrete was destroyed. Concrete in composite links can delay web buckling and improve the seismic performance of the structure. The results obtained from the composite specimens reveal that a portion of the link shear capacity may be assigned to concrete in design procedure.

According to the test results for specimens 3 and 4, the distance between shear reinforcements increased the shear capacity insignificantly. This can be very well observed by comparison between hysteretic diagrams of these two samples. Ultimate displacement of Sample 3 with lower stirrup space is higher than that of Sample 4.

References

AISC (2002), "Seismic provisions for structural steel buildings", American Institute of Steel Construction.

AISC (2005), "Seismic provision for structural steel building", American Institute of Steel Structure.

Applied Technology Council (ATC) (1992), "Guidelines for seismic testing of components of steel structures", Report-24.

ANSYS Ver .11 (2006), User Manual and Theory, Swan Analysis Systems Inc.

Begum, M., Driver, R.G. and Elwi, A.E. (2007), "Finite-element modeling of partially encased composite columns using the dynamic explicit method", *J. Struct. Eng.*, **133**(3), 326-334.

Bruneau, M. and Zahrai, M. (1999), "Seismic performance of diaphragms in slab-on-girder steel bridges", *J. Struct. Eng.*, **125**(9), 987-996.

Bruneau, M. and Sarraf, M. (2000), "Innovative application of ductile system in seismic retrofit of deck-truss bridges", *12th WCEE*, 1350-1358.

Bruneau, M., Sarraf, M., Zahrai, S.M. and Alfawakhiri, F. (2002), "Displacement-based energy dissipation systems for steel bridges diaphragms", *J. Constr. Steel Res.*, **58**(5-8), 801-817.

Chicoine, T., Trembla, R. and Massicotte, B. (2002), "Finite element modelling and design of partially encased composite columns", *Steel Compos. Struct.*, **2**(3), 171-194.

D'Aniello, M. (2006), "Seismic upgrading of RC structure by steel eccentrically bracing (An experimental and numerical study)", *Pollack Periodica*, **1**(2), 17-32.

Dusicka, P., Itani, A.M. and Buckle, I.G. (2002), "Cyclic behavior of shear links and tower shaft assembly of San Francisco-Oakland Bay bridge tower", *Technical report CCEER 02-06, Center for Civil Eng. Earthq. Res.*

El-Tawil, S. and Deierlein, G.G. (1999), "Strength and ductility of concrete encased composite columns", *J. Struct. Eng.*, **125**(9), 1009-1019.

Fehling, E., Pauli, W. and Bauwkamp, J.C. (1992), "Use of vertical shear link in eccentrically braced frames", *10th World conference on Earthquake Engineering*, Madrid.

Ghobarah, A. and Abou Elfath, H. (2001), "Rehabilitation of a reinforced concrete frame using eccentric steel", *Eng. Struc.*, **23**(7), 745-755.

Itani, A.M. (1997), "Cyclic behavior of Richmond-San Rafael tower links", *Technical report CCEER 97-4, Center for Civil Eng. Earthq. Res.*

Kasai, K. and Popov, E.P. (1986), "General behavior of WF steel shear link beams", *J. Struc. Eng.*, **112**(2), 362-382.

Mander, J.B., Priestley, M. and Park, R. (1988), "Theoretical stress-strain model for confined concrete", *J. Struct. Eng.*, **114**(8), 1804-1826.

McDaniel, C.C., Uang, C.-M. and Seible, F. (2003), "Cyclic testing of built-up steel shear links for the new bay bridge", *J. Struct. Eng.*, **129**(6), 801-809.

Okazaki, T., Arce, G., Ryu, H.-C. and Engelhardt, M.D. (2005), "Experimental study of local buckling, overstrength, and fracture of links in eccentrically braced frames", *J. Struct. Eng.*, **131**(10), 1526-1535.

Richards, P.W. and Uang, C.-M. (2006), "Testing protocol for short links in eccentrically braced frames", *J.*

Struct. Eng., **132**(8), 1183-1191.

Ricles, J.M. and Popov, E.P. (1987), "Dynamic analysis of seismically resistant eccentrically braced frames", *Report No. 87/07, Earthq. Eng. Res. Center*, University of California, Berkeley.

Ricles, J.M. and Popov, E.P. (1987), "Experiments on eccentrically braced frames with composite floors", *Report No. 87/06, Earthq. Eng. Res. Center*, University of California, Berkeley.

Roeder, C.W. and Popov, E.P. (1977), "Inelastic behavior of eccentrically braced steel frames under cyclic loading", *Report No. 77/18, Earthq. Eng. Res. Center*, University of California, Berkeley.

Seki, M., Katsumata, H., Uchida, H. and Takeda, T. (1988), "Study on earthquake response of two-storied steel frame with y-shaped braces", *Proceedings 9th World Conference on Earthquake Engineering*, Tokyo-Kyoto, Japan, 65-70.

Shayanfar, M., Rezaeian, A. and Taherkhani, S. (2008), "Assessment of the seismic behavior of eccentrically braced frame with double vertical link (DV-EBF)", *14th World Conference on Earthquake Engineering*, Beijing, China.

Shinabe, Y. and Takahashi, Y. (1995), "The present state of eccentric brace design in Japan", *4th Pacific Structural Steel Conference*, **1**, 813-820.

Szmigiera, E. (2007), "Influence of concrete and fibre concrete on the load-carrying capacity and deformability of composite steel-concrete columns", *J. Civil Eng. Manag.*, **13**(1), 55-61.

Uy, B. (2001), "Axial compressive strength of short steel and composite columns fabricated with high strength steel plate", *Steel Compos. Struct.*, **1**(2), 171-194.

Vetr, M.G. (1998), "Seismic behavior, analysis and design of eccentrically braced frames with vertical shear links", Ph. D. thesis. University of technology Darmstadt w. Germany.

Wakabayashi, M. (1989), "Steel structure",.maruzen, Tokyo, Japan, 399-403.

Zhao, Q. and Astaneh-Asl, A. (2007), "Seismic Behavior of Composite Shear Wall Systems and Application of Smart Structures Technology", *Steel Struct.*, **7**, 69-75.